Hindawi Publishing Corporation
International Journal of Photoenergy
Volume 2015, Article ID 626201, 6 pages
http://dx.doi.org/10.1155/2015/626201

Research Article

Investigating the Effect of Thermal Annealing Process on the Photovoltaic Performance of the Graphene-Silicon Solar Cell

Lifei Yang, Xiaolei Wu, Xin Shen, Xuegong Yu, and Deren Yang

State Key Lab of Silicon Materials, Department of Materials Science and Engineering, Zhejiang University, Hangzhou 310027, China

Correspondence should be addressed to Deren Yang; mseyang@zju.edu.cn

Received 2 October 2014; Revised 17 December 2014; Accepted 6 January 2015

Academic Editor: Wayne A. Anderson

Graphene-silicon (Gr-Si) Schottky solar cell has attracted much attention recently as promising candidate for low-cost photovoltaic application. For the fabrication of Gr-Si solar cell, the Gr film is usually transferred onto the Si substrate by wet transfer process. However, the impurities induced by this process at the graphene/silicon (Gr/Si) interface, such as H_2O and O_2, degrade the photovoltaic performance of the Gr-Si solar cell. We found that the thermal annealing process can effectively improve the photovoltaic performance of the Gr-Si solar cell by removing these impurities at the Gr/Si interface. More interestingly, the photovoltaic performance of the Gr-Si solar cell can be improved, furthermore, when exposed to air environment after the thermal annealing process. Through investigating the characteristics of the Gr-Si solar cell and the properties of the Gr film (carrier density and sheet resistance), we point out that this phenomenon is caused by the natural doping effect of the Gr film.

1. Introduction

The fascinating properties of graphene (Gr), such as high carrier mobility, high optical transparency, and tunable work function, make it an attractive candidate for application in optoelectronic and photovoltaic devices [1–4]. Recently, there is growing interest in incorporating Gr with silicon (Si) to develop graphene-silicon (Gr-Si) solar cell, in which the Gr film forms Schottky junction with Si functioning for carrier separation [5, 6]. To form Gr-Si Schottky junction, the Gr film can be simply placed onto a Si substrate at room temperature by the traditional wet transfer process [7] and the high temperature diffusion process needed for forming p-n junction is eliminated. Hence, the Gr-Si solar cell is considered as a potential low-cost alternative to the conversional crystallize silicon p-n junction solar cell. However, the impurities induced during the wet transfer process at the graphene/silicon (Gr/Si) interface, such as H_2O and O_2 (H_2O/O_2), may degrade the performance of the Gr-Si devices [8].

In this work, we demonstrate that the photovoltaic performance of the Gr-Si solar cell can be improved effectively by thermal annealing process. Particularly, the efficiency of the Gr-Si solar cell is enhanced by about ten times due to the reducing of the series resistance of the solar cell, which is believed to be resulting from the removing of the trapped H_2O/O_2 at the Gr/Si interface. More interestingly, when exposed to air ambient after the thermal annealing process, the efficiency of the Gr-Si solar cell is found to be improved furthermore. By systematically investigating the characteristics of the Gr-Si solar cell and the properties of the Gr film (carrier density and sheet resistance), we point out that the further performance enhancement for the Gr-Si solar cell is caused by the natural p-type doping of the Gr film due to the reabsorption of H_2O/O_2 molecules on the Gr film surface.

2. Experiments

2.1. Gr Preparation, Transfer, and Characterization. Monolayer Gr film was produced by a copper (Cu) catalyzed low pressure chemical vapor deposition (LPCVD) method at 1000°C, using CH_4 (20 sccm) as the carbon source and H_2 (40 sccm) as the reduction gas. Traditional PMMA-assisted wet transfer process was used for Gr film transfer. The PMMA dissolved in chlorobenzene was spin coated on Gr/Cu film

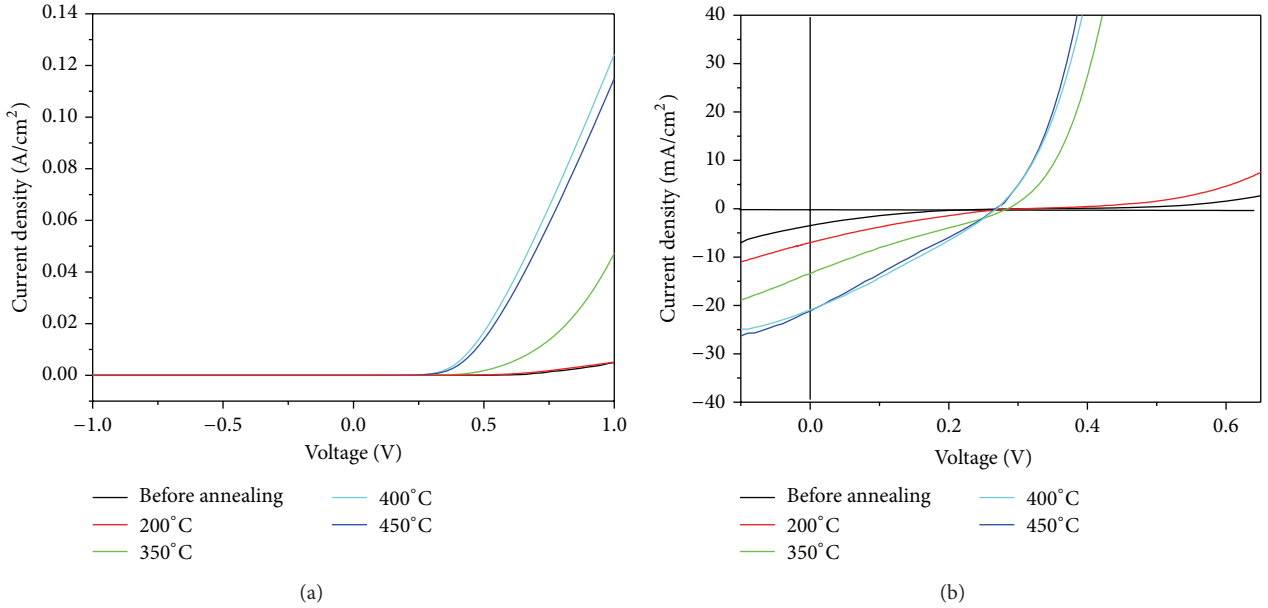

Figure 1: The current density-voltage (*J-V*) curves in dark (a) and under illumination (b) of the Gr-Si solar cell before annealing and after thermal annealing processes at different temperatures.

at 4000 rpm for 30 s, followed by curing at 200°C for 10 min. After the Gr on the backside of the Cu foil was removed by exposing to ozone for 10 min, the Cu foil was etched away by a mixture of $FeCl_3$ and HCl solution to get PMMA/Gr film. The PMMA/Gr film was rinsed in DI water for 3 times and then transferred onto the target substrate, and finally the PMMA was removed using acetone. The electrical properties of the Gr film (sheet resistance and carrier density) were measured with a Hall system (Lakeshore).

2.2. Gr-Si Solar Cell Fabrication and Performance Evaluation. N-type ⟨100⟩ Czochralski (CZ) Si wafer with resistivity of 1–3 Ω·cm was used as a substrate for the device fabrication. The Si wafer was cleaned by the IMEC clean process, and then it was exposed to ambient air for two hours before use. Subsequently, a monolayer Gr film was transferred onto the Si substrate with a traditional PMMA-assisted wet transfer process. Afterwards, the front contact was formed by applying Ag paste around the Gr film to enclose a nearly square window as the device-active area (~9 mm^2) and the back contact was made by scratching the InGa eutectic alloy at the Si backside, thus forming a complete Gr-Si solar cell. After measuring the current density-voltage (*J-V*) characteristics of the resulting Gr-Si solar cell both in dark and under illumination, the Gr-Si solar cell was subjected to thermal annealing processes at given temperatures (200°C, 350°C, 400°C, and 450°C) for one hour under forming gas. After each thermal annealing process, the *J-V* curves of the Gr-Si solar cell were measured again and the InGa eutectic alloy at the backside of Si was removed completely before applying next thermal annealing process. The measurement system used here consists of a Keithley 2400 source meter and a solar simulator calibrated by a standard Si solar cell to provide a standard AM 1.5G illumination with intensity of 100 mW/cm^2.

3. Results and Discussion

Figure 1 shows the *J-V* curves of the Gr-Si solar cell in dark and under illumination before annealing and after thermal annealing processes at different temperatures. It can be seen that the thermal annealing process improves the device characteristics both in dark and under illumination. In dark, the forward current of the Gr-Si diode increases progressively as the annealing temperature increases from 200°C to 450°C and the turn-on voltage of the Gr-Si diode slightly decreases. Under illumination, the photovoltaic performance of the solar cell is progressively enhanced as the annealing temperature varying from 200°C to 450°C. Particularly, the short circuit current density (J_{SC}), the fill factor (FF), and the efficiency of the solar cell are increased from 3.5 mA/cm^2 to 21.2 mA/cm^2, from 0.13 to 0.25, and from 0.14% to 1.45%, respectively (see Table 1). It is also found that the efficiencies of the Gr-Si solar cell are nearly equal after thermal annealing process at 400°C and 450°C. Therefore, the optimal thermal annealing temperature for the Gr-Si solar cell is about 400°C. Similar measurements have been taken on three Gr-Si solar cell samples and the trends reported here reproduced on all the samples. Figure 2 shows the evolution of series resistance (R_s) of the Gr-Si solar cell with the thermal annealing temperature. It can be seen that the R_s of the Gr-Si solar cell is largely reduced as the annealing temperature varying from 200°C to 450°C. Particularly, the R_s of the solar cell decreases from ~70 Ω·cm^2 before annealing to ~4 Ω·cm^2 after thermal annealing at 400°C. This causes the increase of the J_{SC} and FF of the solar cell as shown in Table 1.

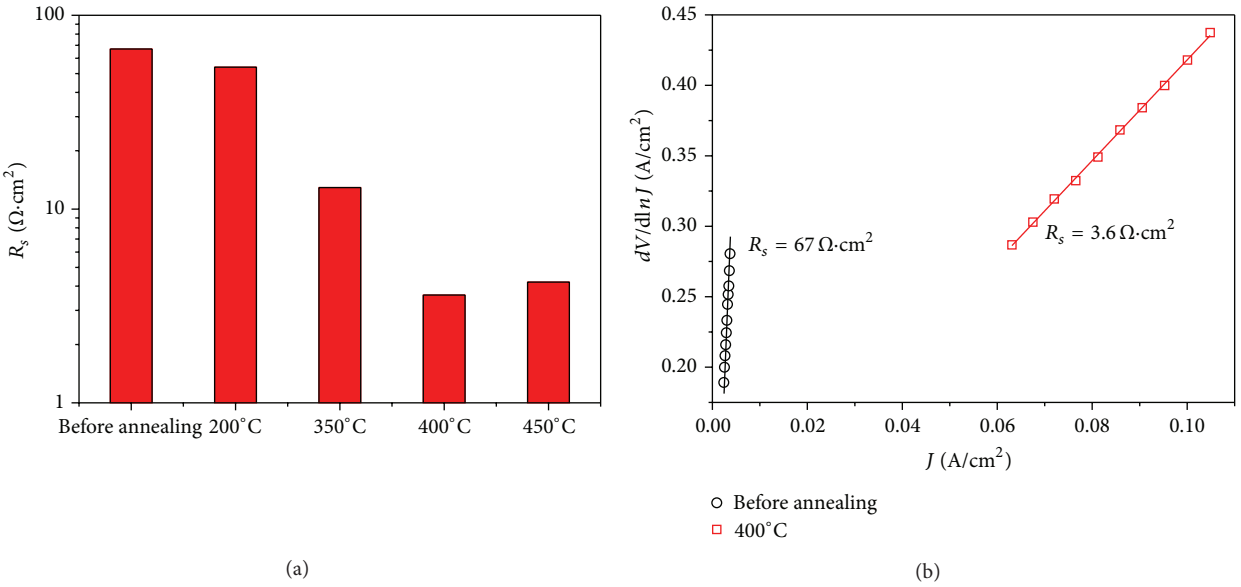

FIGURE 2: (a) The evolution of series resistances (R_s) of the Gr-Si solar cell with thermal annealing temperature. (b) Typical examples showing how the R_s values of the Gr-Si solar cell are extracted [5].

TABLE 1: The photovoltaic parameters of Gr-Si solar cell before annealing and after thermal annealing processes at different temperatures.

Annealing temperature	V_{OC} (V)	J_{SC} (mA/cm^2)	FF	Eff.
Before annealing	0.32	3.5	0.13	0.14%
200°C	0.31	7.0	0.18	0.39%
350°C	0.29	13.4	0.23	0.89%
400°C	0.27	20.9	0.26	1.49%
450°C	0.27	21.2	0.25	1.45%

The R_s of the Gr-Si solar cell is composed of four parts:

$$R_s = R_{\text{C-MG}} + R_{\text{C-MS}} + R_{\text{Gr}} + R_{\text{Si}}, \quad (1)$$

where $R_{\text{C-MG}}$ is the contact resistance between the top electrode and the Gr film, $R_{\text{C-MS}}$ is the contact resistance between the bottom electrode and the Si substrate, R_{Gr} and R_{Si} represent the body resistance of the Gr film and the Si substrate, respectively. For our Gr-Si solar cell, the Si substrate maintains a negligible resistance (e.g., if the resistivity of the Si substrate is 3 Ω·cm and the thickness of the Si substrate is 0.5 mm, then the R_{Si} is 0.15 Ω·cm^2). $R_{\text{C-MS}}$ can also be ignored if typical low-resistivity metal-Si contact such as Ti/Au, Ti/Pd/Ag, or InGa is used. Thus, the R_s can be simplified as

$$R_s = R_{\text{C-MG}} + R_{\text{Gr}}. \quad (2)$$

It is reported that the thermal annealing process can reduce the contact resistance between the metal electrode and the Gr film [9]. To verify the impact of $R_{\text{C-MG}}$ on R_s, another Gr-Si solar cell is fabricated which is subject to 400°C annealing process firstly and then applying the top and bottom

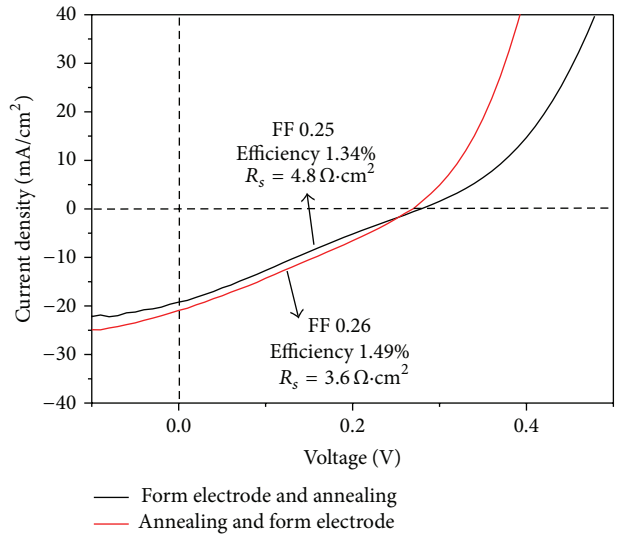

FIGURE 3: The illuminated *J-V* curves of the Gr-Si solar cells fabricated by different process sequence.

electrodes. Figure 3 compares the photovoltaic performance of the Gr-Si solar cells fabricated by these two different approaches. It can be seen that they have similar values of R_s, FF, and efficiency. This result indicates that the $R_{\text{C-MG}}$ is not the main factor determining the R_s of the Gr-Si solar cell. Thus, the R_s of the Gr-Si solar cell should be determined by the R_{Gr}, which is supposed to be reduced by the thermal annealing process. However, the sheet resistance of the Gr film is found to be largely increased after thermal annealing at 400°C, as will be discussed later. This observation is disagreeing with the fact that the R_s of the Gr-Si solar cell can be reduced by the thermal annealing process. Hence, there

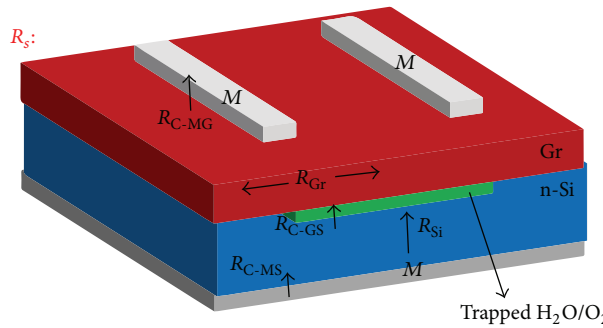

FIGURE 4: Schematic diagraph of the R_s compositions of Gr/Si solar cell. The resistance of the top metal electrode and that of the bottom metal electrode are ignored.

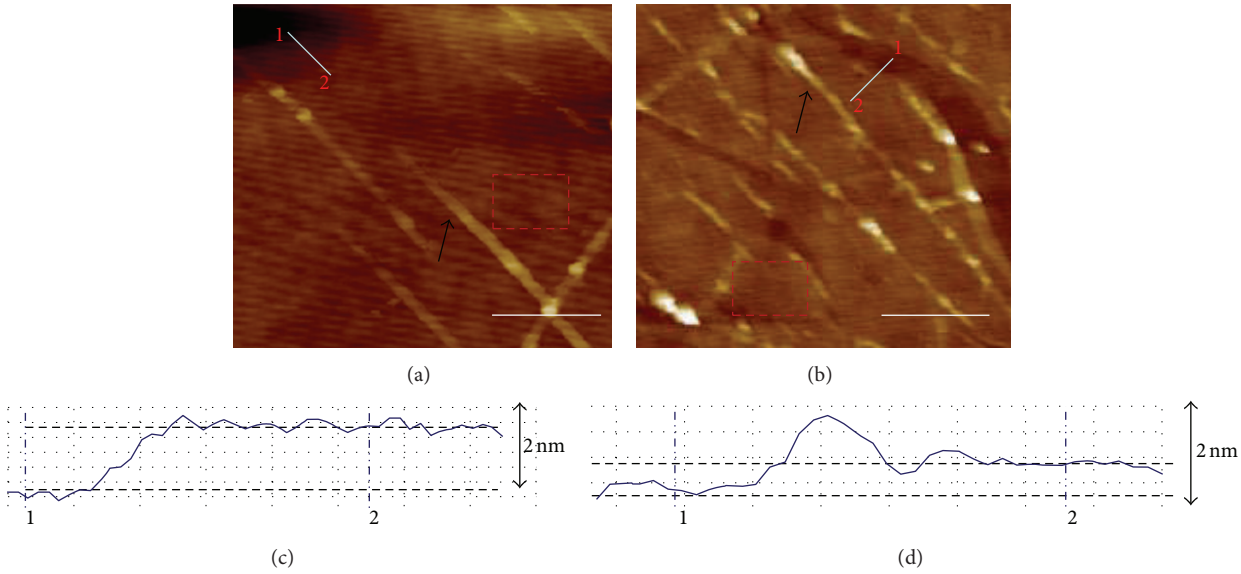

FIGURE 5: AFM images of the Gr film on Si substrate: (a) before annealing; (b) after thermal annealing at 400°C. The height profile of the Gr films along the white line starting from where the Gr film is partly broken (point 1): (c) before annealing; (d) after annealing at 400°C. The root-mean-square (rms) surface roughness is acquired on a scan window highlighted by the red box. The arrows in the AFM images show the corrugation of the Gr film. The scale bars represent 1 μm.

must be another factor that also determines the R_s of the Gr-Si solar cell and the formula of the R_s should be modified as

$$R_s = R_{C\text{-}MG} + R_{C\text{-}MS} + R_{Gr} + R_{Si} + R_{C\text{-}GS}. \quad (3)$$

As shown in Figure 4, we suppose that the $R_{C\text{-}GS}$ is caused by the trapped H_2O/O_2 at the Gr/Si interface, which can block the transport of the carriers from the silicon to the Gr film and thus increase the R_s of the Gr-Si solar cell. The thermal annealing process can remove the trapped H_2O/O_2 at the Gr/Si interface and thus helps to reduce the R_s of the Gr-Si solar cell. Figure 5 shows the AFM images of the Gr film on Si substrate before and after thermal annealing at 400°C, respectively. It can be seen that the height of the Gr film before annealing is about 1.5 nm and the root-mean-square (rms) surface roughness of the Gr film is measured to be 0.54 nm. After thermal annealing at 400°C, these values decrease to 0.4 nm and 0.2 nm, respectively. This observation, according to our understanding, is due to the existence of trapped H_2O/O_2 at the Gr/Si interface, which can be removed by the thermal annealing process.

Interestingly, the efficiency of the Gr-Si solar cell is found to be improved, furthermore, when exposed to air ambient after the thermal annealing process. Exposure to air ambient for 100 hours makes the V_{OC}, J_{SC}, FF, and the efficiency of the Gr-Si solar cell increase from 0.27 V to 0.32 V, from 21.2 mA/cm^2 to 22.2 mA/cm^2, from 0.25 to 0.30, and from 1.45% to 2.1%, respectively (see Figure 6). After that, the photovoltaic performance of the Gr-Si solar cell becomes stable and no more improvement can be found as the exposing time increases to 200 hours. Figure 7 shows the electrical properties of the Gr film before and after thermal annealing at 400°C and their evolution with the exposing time after the thermal annealing process. It can be found that the sheet resistance of the Gr film increases largely after thermal annealing at 400°C because of a dramatic decrease of its carrier density. Then, after exposure to air ambient,

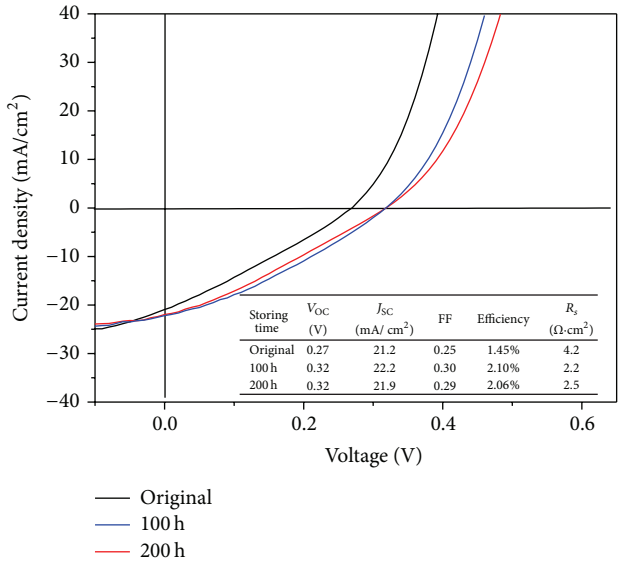

Figure 6: The evolution of the photovoltaic performance of the Gr-Si solar cell with exposing time after thermal annealing process.

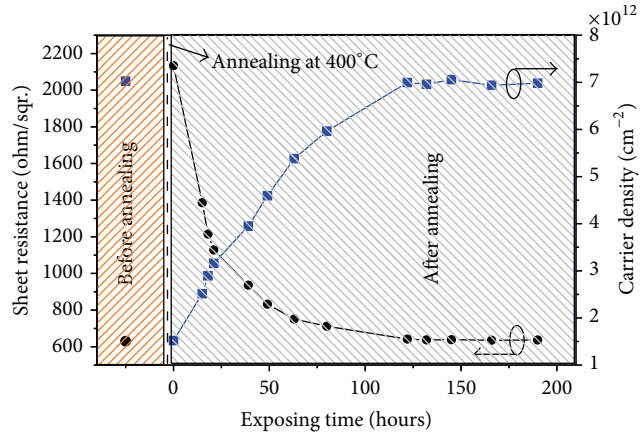

Figure 7: The electrical properties of Gr film before and after annealing at 400°C and their evolution with the exposing time after thermal annealing process.

its sheet resistance and carrier density recover slowly and finally return to their original levels after ~120 hours. These observations can be explained by the natural doping effect of the Gr film and its effect on the photovoltaic performance of the Gr-Si solar cell (see Figure 8). Owing to the linear energy band structure of the Gr film, the change of the work function of the Gr film (ΔW_{Gr}) can be related to the change of its carrier density (Δn) as (1) [10]. Consider

$$\Delta W_{Gr} = \frac{h v_F}{2\pi} \sqrt{\pi \Delta n}, \quad (4)$$

where v_F is the Fermi velocity (1.1×10^6 m·s^{-1}), h is the Planck Constant (6.626×10^{-34} J·s), and n is the carrier density of the Gr film. The V_{OC} of the Gr-Si Schottky junction solar cell is determined by the difference between the work function of the Gr film and that of the silicon substrate. The increasing of the work function of the Gr film will cause the increasing of the V_{OC} of the Gr-Si solar cell. The as-grown Gr film is p-typed and doped by the H_2O/O_2 molecular system that is absorbed onto the surface of the Gr film [11]. After the Gr-Si solar cell is subjected to thermal annealing at 400°C, the H_2O/O_2 trapped at the Gr/Si interface and that absorbing into the Gr film surface are all removed. This causes the reducing of the R_s of the Gr-Si solar cell as discussed before and the decreasing of the work function of the Gr film, which makes the V_{OC} of the Gr-Si solar cell decrease from 0.32 V to 0.27 V. After that, the Gr film is redoped because of the reabsorbing of H_2O/O_2 into its surface when exposed to air environment. This causes the recovery of the work function of the Gr film, making the V_{OC} of the Gr-Si solar cell recover to 0.32 V. As for the R_s of the Gr-Si solar cell, the reabsorbing H_2O/O_2 cannot enter the Gr/Si interface because the Gr film is now tightly contacting with the silicon substrate after the thermal annealing process. Hence, the R_s of the Gr-Si solar cell decreases further from ~4 Ω·cm^2 to 2.5 Ω·cm^2 because the sheet resistance of the Gr

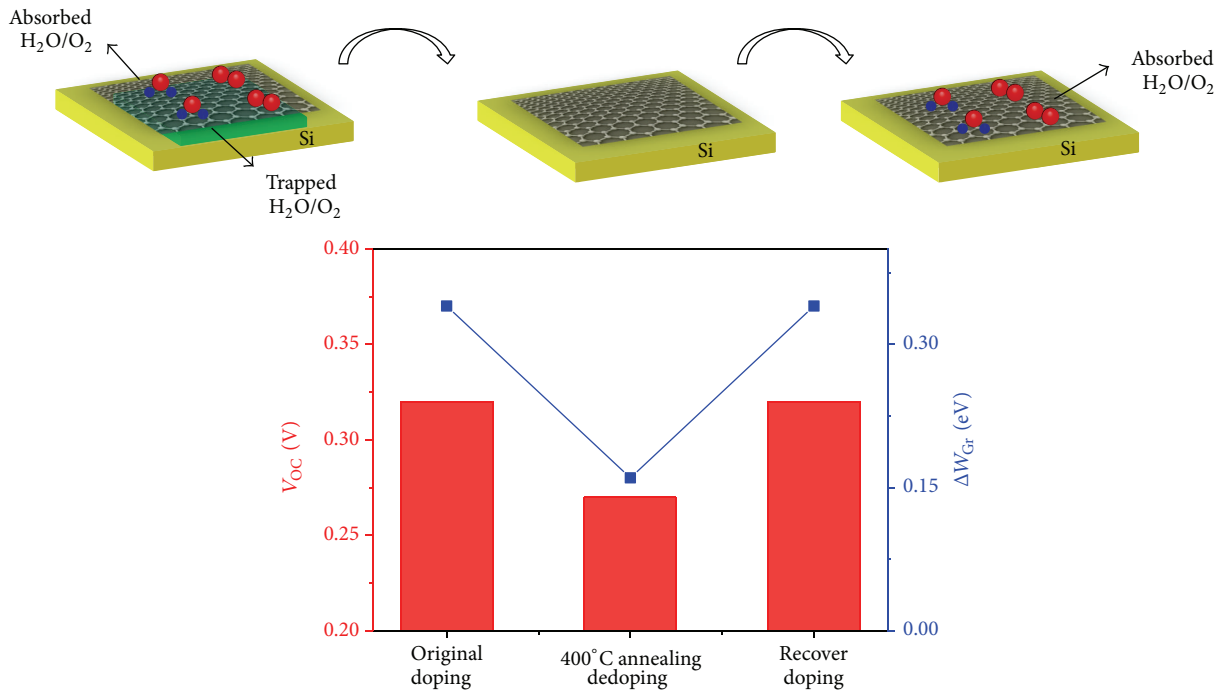

Figure 8: The nature doping effect of the Gr film and its impact on the V_{OC} of the Gr-Si solar cell.

film decreases from ~2000 Ω/□ to ~600 Ω/□. Finally, as the natural doping effect recovers completely, the performance of the Gr-Si solar cell becomes stable.

4. Conclusions

In summary, we found that the thermal annealing process can improve the photovoltaic performance of the Gr-Si solar cell effectively through removing the rapped H_2O/O_2 at the Gr/Si interface. The optimal annealing temperature is about 400°C. When exposed to the air environment after the annealing process, the photovoltaic performance of the Gr-Si solar cell can be improved furthermore thanks to the natural doping effect of the Gr film.

Conflict of Interests

The authors declare that there is no conflict of interests regarding the publication of this paper.

Acknowledgment

This work is supported by the National Natural Science Foundation of China (nos. 61422404 and 61274057).

References

[1] K. S. Novoselov, V. I. Fal'Ko, L. Colombo, P. R. Gellert, M. G. Schwab, and K. Kim, "A roadmap for graphene," *Nature*, vol. 490, no. 7419, pp. 192–200, 2012.

[2] T. Mueller, F. Xia, and P. Avouris, "Graphene photodetectors for high-speed optical communications," *Nature Photonics*, vol. 4, no. 5, pp. 297–301, 2010.

[3] L. Britnell, R. V. Gorbachev, R. Jalil et al., "Field-effect tunneling transistor based on vertical graphene heterostructures," *Science*, vol. 335, no. 6071, pp. 947–950, 2012.

[4] X. An, F. Liu, Y. J. Jung, and S. Kar, "Tunable graphene-silicon heterojunctions for ultrasensitive photodetection," *Nano Letters*, vol. 13, no. 3, pp. 909–916, 2013.

[5] X. Li, H. Zhu, K. Wang et al., "Graphene-on-silicon schottky junction solar cells," *Advanced Materials*, vol. 22, no. 25, pp. 2743–2748, 2010.

[6] Y. Ye and L. Dai, "Graphene-based Schottky junction solar cells," *Journal of Materials Chemistry*, vol. 22, no. 46, pp. 24224–24229, 2012.

[7] X. Li, W. Cai, J. An et al., "Large-area synthesis of high-quality and uniform graphene films on copper foils," *Science*, vol. 324, no. 5932, pp. 1312–1314, 2009.

[8] G. S. Kim, D. J. Kim, N. W. Park et al., "Effect of annealing of graphene layer on electrical transport and degradation of Au/graphene/n-type silicon Schottky diodes," *Journal of Alloys and Compounds*, vol. 612, pp. 265–272, 2014.

[9] O. Balci and C. Kocabas, "Rapid thermal annealing of graphene-metal contact," *Applied Physics Letters*, vol. 101, no. 24, Article ID 243105, 2012.

[10] J. B. Bult, R. Crisp, C. L. Perkins, and J. L. Blackburn, "Role of dopants in long-range charge carrier transport for p-type and n-type graphene transparent conducting thin films," *ACS Nano*, vol. 7, no. 8, pp. 7251–7261, 2013.

[11] D.-W. Shin, H. M. Lee, S. M. Yu et al., "A facile route to recover intrinsic graphene over large scale," *ACS Nano*, vol. 6, no. 9, pp. 7781–7788, 2012.